

Electrophysiological, pharmacological and molecular profile of the transiently outward rectifying conductance in neonatal rat sympathetic preganglionic neurones *in vitro*.

A. D. WHYMENT & *D. SPANSWICK NeuroSolutions Ltd., Coventry, UNITED KINGDOM

NEUROSolutions LTD.

www.nsolns.com

1 INTRODUCTION

Outward currents through potassium (K^+) channels are the primary means by which excitable cells oppose membrane excitability. Several distinct types of K^+-mediated conductances have been identified in sympathetic preganglionic neurones (SPNs). One such conductance: the transient outward rectifying conductance (I_{TOR}) or A-like conductance is a hallmark of SPN and is used as an identifiable, characteristic electrophysiological feature of these neurones. In SPN this conductance is prolonged, lasting for hundreds of milliseconds to seconds and is thought to play a key role in the regulation of SPN firing frequency.

At the molecular level, voltage-gated K^+ channels (Kv) mediate these rapidly inactivating outward currents. Kv channels are composed of two classes of subunits; the α-subunit, which forms the channel pore and auxiliary (β) subunits. The Kv α-subunit is a typical six transmembrane spanning protein, with unusually large intracellular N- and C-termini loops. These confer control of the activity-dependent regulation of channel closure (channel inactivation) and are the site of protein-protein interactions (interaction with cytoplasmic β-subunits) within the channel.

Here, a multidisciplinary electrophysiological, pharmacological and molecular single-cell rt-PCR approach was used to investigate the kinetics, pharmacological profile and putative K^+ channel subfamily subunits underlying the transient outward rectifying conductance expressed in SPN.

2 METHODS

***In vitro* methods**:
Neonatal wistar-kyoto rats (6-14 days) were terminally anaesthetised with enflurane (4% in O_2), cervically dislocated and decapitated and whole-cell patch clamp recordings made from SPN in the intermediolateral cell column (IML) of 400 µM transverse thoracolumbar spinal cord slices as described previously (Logan *et. al.* 1996). All experiments were performed at room temp.

Single-cell RT-PCR methods:
The neuronal harvest and single-cell RT-PCR from SPN was carried out as described in detail previously (van den Top *et al.*, 2004). Briefly, the cytoplasm of an SPN was gently aspirated under visual control into a patch-clamp recording electrode. The contents of the electrode were subsequently expelled into a microtube and reverse transcribed for 60 min at 42 °C. Three prime end amplification (TPEA) was performed using methods described in detail previously (Dixon *et al.*, 1998). Samples of amplified cDNA were diluted 1:10 and subjected to hot-lid PCR. Following an initial 4 min denaturing step (95 °C), each PCR cycle consisted of 30 s denaturing (94 °C), 30 s annealing (60 °C) and 20 s extension (72 °C) then 5 min at 72 °C. Direct sequencing was performed to confirm the identity of all amplified products.

Steady state inactivation and activation data were fit after normalisation to a single Boltzmann function;

$$G/Gmax = 1 + \exp[(V\text{-}Vh)/k]^{-1}$$

(where Gmax is the maximal conductance, *Vh* is the half-inactivation potential and *k* the slope factor)
by non linear regression using Microcal Origin 7. The decay of the current was fitted by the following equation:

$$I(t) = \{Is(\exp(-t/\tau s))\} + \{If(\exp(t/\tau f))\} + Io$$

(where *I(t)* is the total current at time t, *Is* and *If* are the initial amplitudes of the two components relating to the slow (τs) and fast (τf) decay time constants, and the non-inactivating residual current (*Io*).

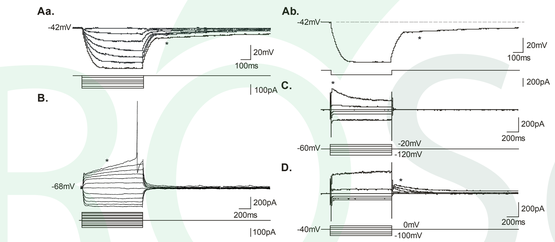
The following drugs were used at the final concentrations indicated: 4-aminopyridine (4-AP, 0.1-5 mM); BDS-II, 1µM; Dendrotoxin-I (DTX-I, 200 nM); Pandinotoxin-Kα (PiTx-Kα, 50 nM); Tityustoxin-Kα (TiTx-Kα, 100 nM), all from Sigma and Phrixotoxin-2 (PaTx-2, 1-10 µM); Tetrodotoxin (TTX, 500 nM) from Alomone Laboratories, Israel.

Name	Gene Accession Number	Primer Sequence (+), sense; (-), antisense	Product length (bp)
Kv 1.4	NM_012971	(+) 5' - GCACCAATCAGTTCAATGAC - 3' (–) 5' - CAGGAATCGTGTGCTGTTAT - 3'	111
Kv 1.5	NM_145983	(+) 5' - GGCAGACTGGCACCAGTGAA - 3' (–) 5' - ACGGCTCCTGCGTCATGGAA - 3'	161
Kv 3.4	X62841	(+) 5' - CAGAGGATGCGTGCAATAGC - 3' (–) 5' - CTAGGCGTGCCTCAGACACA - 3'	144
Kv 4.1	U89873	(+) 5' - GCTGCTGTCATACCAATGTG - 3' (–) 5' - GCTCTTGCTGGATGTTAGTC - 3'	168
Kv 4.2	NM_031730	(+) 5' - AATTGGCACAGGTCTGAGAG - 3' (–) 5' - CCTTCTTGCTTGGCTGTCTT - 3'	111
Kv 4.3	NM_031739	(+) 5' - CTAGACCTGGCCTCACGATT - 3' (–) 5' - CTACTTGGCCTACCTGCTAA - 3'	129
Kvβ1	X70662	(+) 5' - CTCGCACCGCTCTCTGCTCATT - 3' (–) 5' - GGCCAGCCTGGCTTCTATTG - 3'	175
Kvβ2	X76724	(+) 5' - GAGCCACTTAAGCTGCATGA - 3' (–) 5' - GTGGTAGCAACAGCAGGAGC - 3'	143
Kvβ3	NM_031652	(+) 5' - CCGGCTTCGAGTAGCGATTC - 3' (–) 5' - ATGAGCAGAGCGGTGCGAGA - 3'	157
KChIP1	NM_014592	(+) 5' - GGAGAGGCAGCAACTAACAT - 3' (–) 5' - TGATCGTAGGTGCTAGTGTG - 3'	136
KChIP2	AB040031	(+) 5' - GCAGGAGACCTTCTGTCTAA - 3' (–) 5' - GGCAAGAGTAGGCAAGTCAA - 3'	163
KChIP3	AB043892	(+) 5' - CTGAGAGTCCATGCGTGTTC - 3' (–) 5' - GCCTTGGCTTCTCACAGGAT - 3'	250
NCS-1	NM_024366	(+) 5' - GTTGTTAACGAGGCCTGCTA - 3' (–) 5' - CGGAGCACAGTATCTGAGAA - 3'	187
DPP6	NW047685	(+) 5' - ACAGGTCCATCATCGGATTC - 3' (–) 5' - AGGTCTCAAGCGTGGTTAGT - 3'	107

Gene-specific primers used for single-cell RT-PCR.

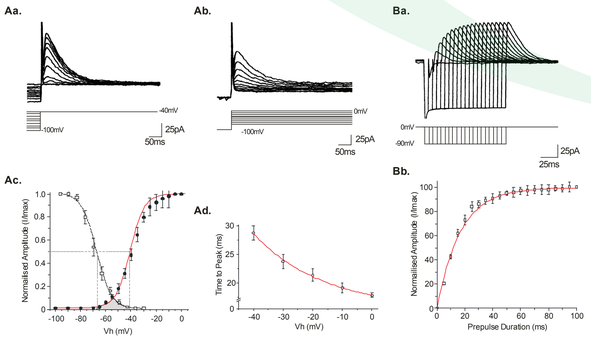
3 Identification of I_{TOR} in SPN

A, Superimposed (a) and a single membrane response (b) illustrating I_{TOR} as a delayed return to resting membrane potential of the responses to hyperpolarising current injection (*). **B**. Superimposed membrane responses to current injection showing I_{TOR} observed as a delay in reaching threshold of the membrane response to depolarising current injection. **C**. Superimposed samples of a continuous whole-cell voltage clamp recording. Note the I_{TOR} evoked in response to the largest depolarising voltage step (*). **D.** Note the I_{TOR} tail currents (*) evoked at the offset of the responses to hyperpolarising voltage step commands.



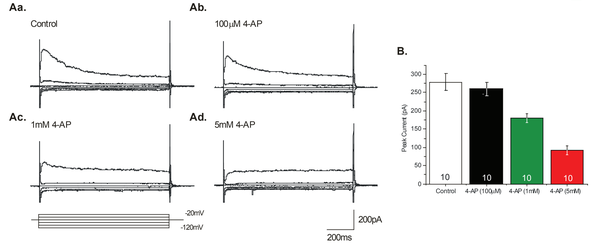
4 Kinetics of I_{TOR} in SPN

A. Steady-state inactivation (a) and activation (b) of the I_{TOR} is voltage-dependent. (c) Plot of the activation (closed circles) and steady-state inactivation (open squares) of I_{TOR} expressed as normalised peak current (I/Imax) as a function of the conditioning potential. (d) Plot of the time to peak of I_{TOR} as a function of the test potential. **B**. Recovery from inactivation of the transient current followed a mono-exponential time-constant. (b) Normalised peak currents (I/Imax) were plotted as a function of recovery interval.



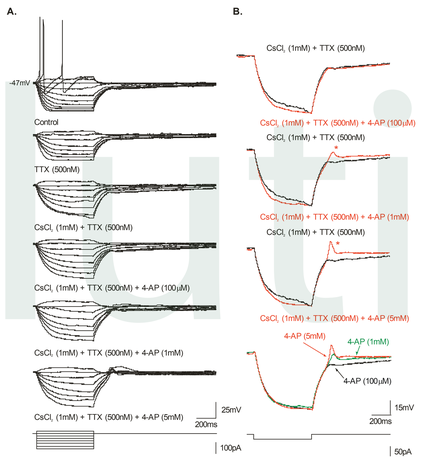
5 Sensitivity of I_{TOR} to 4-AP

A. Superimposed samples of a continuous whole-cell voltage-clamp recording from an SPN at a holding potential of –60 mV showing current responses to a series of depolarising and hyperpolarising rectangular-wave voltage-steps, and the effects of increasing concentrations of 4-aminopyridine. **B.** Plot of the concentration-dependent inhibition of the peak I_{TOR} by 4-AP.



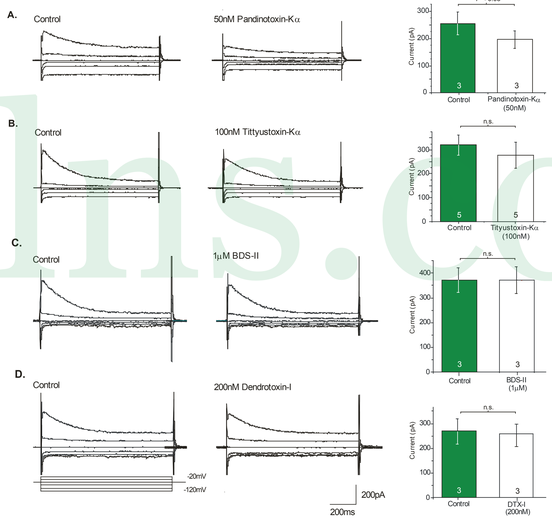
6 Sensitivity of I_{TOR} to 4-AP

A. Superimposed whole-cell current-clamp recordings showing membrane potential responses of an SPN to a series of depolarising and hyperpolarising rectangular-wave current pulses showing the concentration-dependent inhibition of I_{TOR}, observed as the delayed return to rest of membrane responses to hyperpolarising current injection, by 4-AP (**B**).



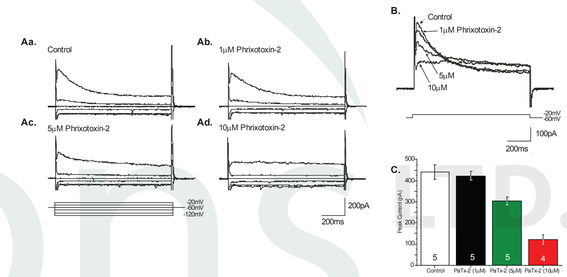
7 Sensitivity of I_{TOR} to toxins

Current-voltage relations evoked from a holding potential of –60 mV showing the sensitivity of I_{TOR} to the rapidly inactivating Kv channel blocker Pandinotoxin-Kα (**A**), the Kv1 channel blocker's Tittyustoxin-Kα (**B**) and Dendrotoxin-I (**D**), the Kv4.3-specific blocker Phrixotoxin-2 and the Kv 3.4 channel specific blocker BDS-II (**C**) with accompanying summary bar charts.



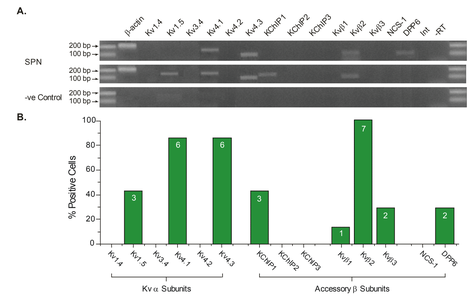
8 Kv4.2/4.3 blocker inhibits I_{TOR}

A. Current-voltage relations evoked from a holding potential of –60 mV showing the sensitivity of I_{TOR} to increasing concentrations of the Kv4.2, Kv4.3-specific blocker Phrixotoxin-2. **B.** Superimposed records from cell shown in A illustrating the concentration-dependent effect of Phrixotoxin-2 on I_{TOR}. **C.** Bar chart illustrating the concentration-dependent inhibition of I_{TOR}.



9 K^+ channel subunit expression

SPN were simultaneously analysed for the expression of Kv1.4, Kv1.5, Kv3.4, Kv4.1, Kv4.2 and Kv4.3 α-subunits, KChIP1, KChIP2, KChIP3, Kvβ1, Kvβ2 and Kvβ3 β-subunits, dipeptidyl aminopeptidase-like protein (DPP6) and neuronal calcium sensor 1 (NCS-1) mRNAs



10 CONCLUSIONS

These data provide the first evidence that the transient outward rectifying current in SPN may be coded for by co-expression of members of the Kv4 subfamily, in association with β-subunits, Kvβ2 being expressed in all cells tested. However, differential expression of accessory β subunits including KChIP 1; Kvβ1 and Kvβ3, and the calcium binding protein DPP6, which may act to modulate channel gating, density and kinetics could underpin the prolonged and variable time-course of this conductance in SPN.

11 REFERENCES

Dixon AK, Richardson PJ, Lee K, Carter NP & Freeman TC. Expression profiling of single cells using 3 prime end amplification (TPEA) PCR, *Nucleic Acids Research* **26(19)** (1998) 4426-4431.

Logan SD, Pickering AE, Gibson IC, Nolan MF & Spanswick D. Electrotonic coupling between rat sympathetic preganglionic neurones *in vitro*, *The Journal of Physiology* **495(2)** (1996) 491-502.

van den Top M, Lee K, Whyment AD, Blanks AM & Spanswick D. Orexigen-sensitive NPY/AgRP pacemaker neurons in the hypothalamic arcuate nucleus. *Nat Neurosci* **7(5)** (2004) 493-494.

© NeuroSolutions Ltd. 2009